Digital Color Restoration of Old Paintings

Michail Pappas and Ioannis Pitas

***Abstract*—Physical and chemical changes can degrade the visual color appearance of old paintings. Five digital color restoration techniques, which can be used to simulate the original appearance of paintings, are presented. Although a small number of color samples is employed in the restoration procedure, simulation results indicate that good restoration quality can be attained.**

***Index Terms*—Enhancement, painting, restoration.**

I. Introduction

Varnish oxidation is a phenomenon that can seriously degrade the visual appearance of old paintings. Dirt, smoke, and other deteriorations can further degrade the appearance of paintings. The result is that colors appear faint and the painting appears brown or black. This is particularly true for icons or church murals, where candle smoke degrades icon colors. In many cases, this degradation can affect the artistic value of a painting. The removal of this oxidation layer is performed by conservation experts. It is a time-consuming process which does not guarantee success. Indeed, the prevailing environmental conditions as well as the chemical properties, which are exhibited by the wide spectrum of different varnishes, render the selection of the appropriate cleaning process quite difficult.

In many cases, a trial and error approach is implemented, where chemical cleaning substances are applied (in small regions, or "samples", of the painting) in order to select the most appropriate substance to be used to clean the entire painting. Digital image processing techniques can be used to simulate color restoration by obtaining an estimation of the original visual appearance of a painting, without extensive chemical cleaning treatment of its surface. In this context, Volterra filters have been utilized to extract the original color information, by utilizing sample painting regions, in the RGB color space, before and after chemical cleaning [1].

Let us assume that several uniformly colored regions of the painting have been cleaned chemically and that the respective digital image patches have been digitized. These constitute the clean color image data set $\mathbf{s}_i, i = 1, \ldots, N$. We can also digitize the same regions before cleaning, or dirty regions having the same paint. These data form the "dirty" image data $\mathbf{x}_i, i = 1, \ldots, N$. Our aim is to find the color transformation $\mathbf{s} = \mathbf{f}(\mathbf{x})$ from these sample data and, subsequently, apply it to the entire image. Most image acquisition systems (e.g. scanner or camera devices) produce RGB data values. However, the RGB color space does not possess perceptional uniformity. That is, numeric color differences between two colors do not accurately represent the perceived color differences [2]. This fact indicates that other color spaces might be more appropriate, at least for the purposes of color image processing applications. The *CIELAB* color space exhibits good correspondence between perceived and actual color differences and device independence [3]. Therefore, we shall work in the CIELAB domain.

The rest of this paper is structured as follows. In Section II the mathematical foundation of the restoration methods is given. Experimental results are presented in Section III. Finally, some conclusions regarding the overall restoration performance are presented in Section IV.

Manuscript received September 2, 1997; revised April 12, 1999. The associate editor coordinating the review of this manuscript and approving it for publication was Dr. Henri Maitre.

The authors are with the Department of Informatics, Aristotle University of Thessaloniki, Thessaloniki, Greece (e-mail: pitas@zeus.csd.auth.gr).

Publisher Item Identifier S 1057-7149(00)01162-3.

II. Restoration Approaches

We assume that a number of color painting patches have already been cleaned. They should have uniform chromaticity and should be representative of the painting colors. Finally, similar colors to the ones of these clean samples should also exist in the dirty or oxidized parts of the painting. Both the clean samples $\mathbf{s}_i, i = 1, \ldots, N$ and $\mathbf{x}_i, i = 1, \ldots, N$ are digitized. Little or no assumptions are made about the painting surface degradation model. In the following, a model function $\mathbf{f}$ is derived for the inverse of the degradation process. It should be clear that a limited number of patches will be utilized in order to approximate this phenomenon. Their number N depends on the number of the representative colors in the painting. The pixel color is denoted by $\mathbf{x} = [x_1 \ x_2 \ x_3]^T$, where x_1, x_2 and x_3 correspond to the L^*, a^* and b^* CIELAB color space coordinates, respectively. If N cleaned regions are available, N corresponding regions from the oxidized part of the image should be selected. Let the vectors $\hat{\mathbf{m}}_{\mathbf{s}_i}$ and $\hat{\mathbf{m}}_{\mathbf{x}_i}$, with $i = 1, \ldots, N$, represent the sample mean of the ith clean and oxidized region, respectively. Furthermore, let $\hat{\mathbf{m}}_{\mathbf{s}}$ and $\hat{\mathbf{m}}_{\mathbf{x}}$ denote the $3 \times N$ sample mean matrices of the clean and oxidized regions, respectively, where

$$\begin{aligned} \hat{\mathbf{m}}_{\mathbf{s}} &= [\hat{\mathbf{m}}_{\mathbf{s}_1} \quad \hat{\mathbf{m}}_{\mathbf{s}_2} \quad \cdots \quad \hat{\mathbf{m}}_{\mathbf{s}_N}] \\ \hat{\mathbf{m}}_{\mathbf{x}} &= [\hat{\mathbf{m}}_{\mathbf{x}_1} \quad \hat{\mathbf{m}}_{\mathbf{x}_2} \quad \cdots \quad \hat{\mathbf{m}}_{\mathbf{x}_N}] \end{aligned} \tag{1}$$

and let $\Delta\hat{\mathbf{m}}$ denote their difference $\hat{\mathbf{m}}_{\mathbf{s}} - \hat{\mathbf{m}}_{\mathbf{x}}$. For each degraded observation $\mathbf{x}$, an estimate $\hat{\mathbf{s}} = \mathbf{f}(\mathbf{x})$ of the reference color $\mathbf{s}$ should be obtained. The *mean square error (MSE)* will be utilized, which is defined as follows:

$$\mathrm{MSE} \simeq \frac{1}{N}\sum_{n=1}^{N} \|\mathbf{s}_n - \hat{\mathbf{s}}_n\|^2 = \frac{1}{N}\sum_{n=1}^{N} (\mathbf{s}_n - \hat{\mathbf{s}}_n)^T (\mathbf{s}_n - \hat{\mathbf{s}}_n) \tag{2}$$

where the operator $\|\cdot\|$ denotes the Euclidean norm.

A. Sample Mean Matching

A straightforward approach can be formulated by classifying first each pixel $\mathbf{x}$ of the oxidized region of the painting, to one of the N color clusters $\hat{\mathbf{m}}_{\mathbf{x}_i}$. The color vector $\mathbf{x}$ is classified to the ith color cluster $\hat{\mathbf{m}}_{\mathbf{x}_i}$, with $i = 1, \ldots, N$ if $\|\mathbf{x} - \hat{\mathbf{m}}_{\mathbf{x}_i}\| < \|\mathbf{x} - \hat{\mathbf{m}}_{\mathbf{x}_j}\|$, for all $i \neq j$. Subsequently, an estimate $\mathbf{s}$ of the original color can be formulated as

$$\hat{\mathbf{s}} = \mathbf{x} + \Delta\hat{\mathbf{m}}_i \tag{3}$$

where $\Delta\hat{\mathbf{m}}_i$ denotes the ith column vector of $\Delta\hat{\mathbf{m}}$. Although this approach is rather simple in terms of modeling the oxidation process, it can perform adequately when the number of color samples N is high.

B. Linear Approximation

Another choice for the approximation function is

$$\mathbf{f}(\mathbf{x}) = (\mathbf{A} + \mathbf{I})\mathbf{x} \tag{4}$$

where $\mathbf{I}$ is the 3×3 identity matrix and $\mathbf{A} = [\mathbf{a}_1 \ \mathbf{a}_2 \ \mathbf{a}_3]^T$ is a 3×3 coefficient matrix. The displacement vector $\mathbf{d} = \mathbf{s} - \mathbf{x}$ can be expressed as

$$\mathbf{d} = \mathbf{A}\mathbf{x}. \tag{5}$$

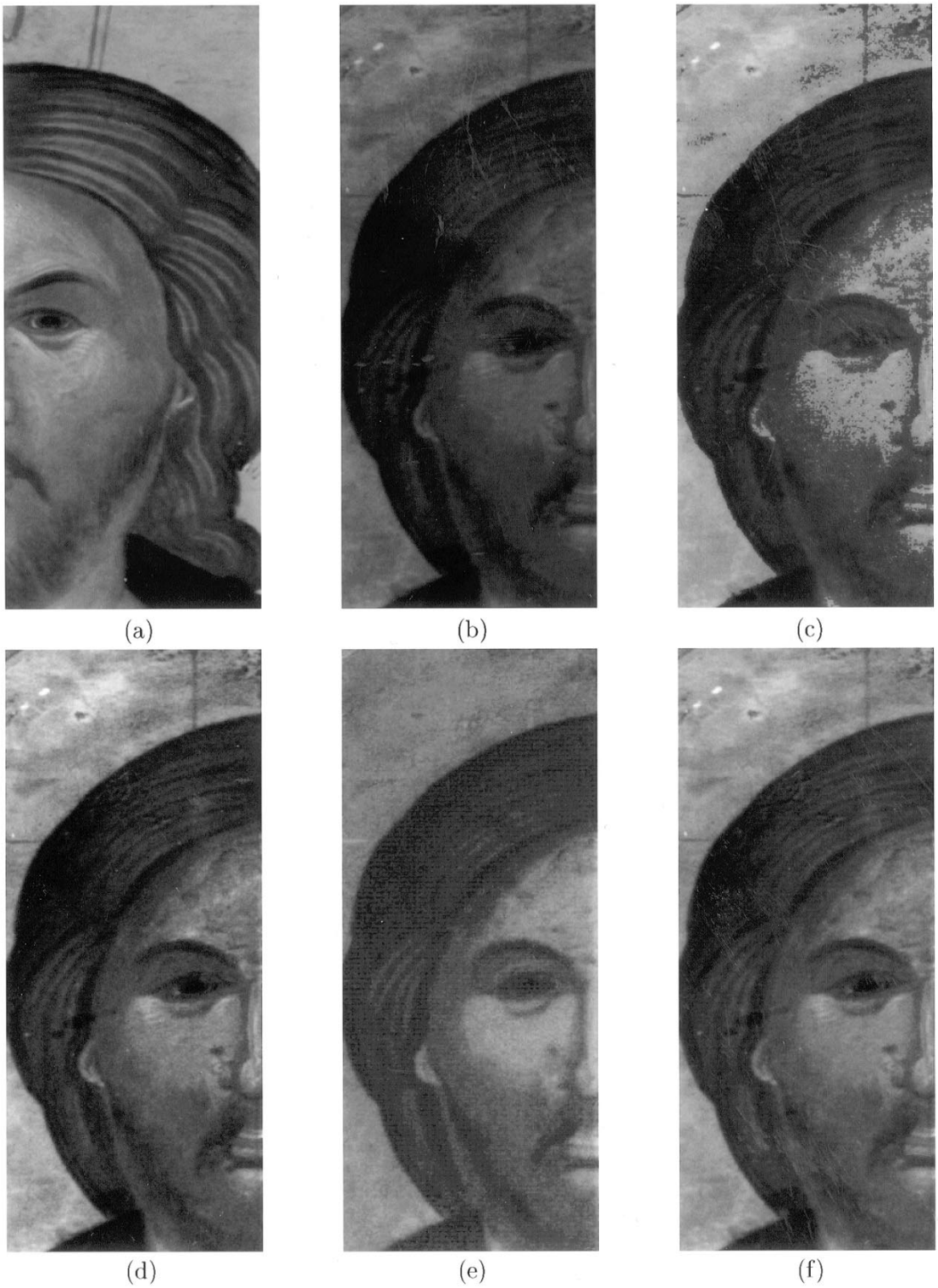

Fig. 1. (a) Clean and (b) oxidized region of the test image. Restoration performance results of the (c) sample mean matching, (d) linear approximation, (e) ICP approximation, and (f) white point transformation methods.

The coefficient matrix $\mathbf{A}$ can be computed by polynomial regression [3]

$$[\{\Delta\hat{\mathbf{m}}\}_{i1} \quad \{\Delta\hat{\mathbf{m}}\}_{i2} \quad \cdots \quad \{\Delta\hat{\mathbf{m}}\}_{iN}]^T = \hat{\mathbf{m}}_{\mathbf{x}}^T \mathbf{a}_i. \tag{6}$$

C. Iterative Closest Point Approximation

The *iterative closest point (ICP)* algorithm is an efficient method for the registration of two 3-D data sets [4]. Let us suppose that two 3-D vector sets $\{\mathbf{x}_i : i = 1, \ldots, N\}$, $\{\mathbf{s}_i : i = 1, \ldots, N\}$ are given, and

TABLE I
MSE COMPARISON OF THE PRESENTED METHODS

Method	*MSE*
Mean sample matching	0.00
Linear approximation	93.21
ICP approximation	369.58
White point	190.37
RBF (one Gaussian per channel)	126.46
RBF (two Gaussians per channel)	88.30

that each vector $\mathbf{x}_i$ corresponds to one vector $\mathbf{s}_i$. The ICP algorithm can be utilized to estimate one 3×3 rotation matrix $\mathbf{R}$ and a 3×1 displacement vector $\mathbf{d}$, in order to provide an approximation function $\mathbf{f}$ of the following form:

$$\mathbf{f}(\mathbf{x}) = \mathbf{R}\mathbf{x} + \mathbf{d}. \tag{7}$$

The number of operations required by the ICP algorithm can be high, since computation cost is, approximately, of the order $O(N^2)$. This presents a serious problem, if the data set size is large. For this purpose, fast implementations of the ICP algorithm can be implemented to perform the matching. Morphological Voronoi tesselations have been utilized to reduce the computational cost, which is associated with the search for the closest point at each iteration [5].

It should be noted that ICP performance depends on the value of the initial registration vector. It is quite probable that ICP may lead to a local minimum.

D. White Point Transformation

Another approach is based on the fact that an object may look different, under different lighting conditions [2]. Assume that a clean sample and its oxidized version are viewed under the same lighting conditions. We assume that if we illuminate a clean sample $\mathbf{s}$ with a "brownish" light source we can obtain the dirty sample $\mathbf{x}$. The light source is characterized by its reference white $\mathbf{w}_{XYZ}$. Thus, the difference in appearance can be attributed solely to the different white point characteristics used by the color transformation required to obtain CIELAB values. In the discussion that follows, vectors with the index XYZ refer to CIEXYZ tristimulus values. Let $\mathbf{s}_{\mathrm{LAB}}$ denote a vector of CIELAB values, which correspond to a clean sample, and let $\mathbf{x}_{XYZ}$ denote a vector that contains the tristimulus values of the corresponding oxidized sample.

For the restoration, a white point vector $\mathbf{w}_{XYZ}$ should be determined which should yield an estimate of the clean sample, that is

$$\hat{\mathbf{s}}_{LAB} = T\{\mathbf{x}_{XYZ}; \mathbf{w}_{XYZ}\} \tag{8}$$

where $T\{\cdot;\cdot\}$ denotes the nonlinear transformation from CIEXYZ to CIELAB. Given the sample mean vectors $\hat{\mathbf{m}}_{\mathbf{x}_{XYZ}}$ of the oxidized samples, the error can be expressed as

$$\mathbf{e} = \hat{\mathbf{m}}_{\mathbf{s}} - T\{\hat{\mathbf{m}}_{\mathbf{x}_{XYZ}}; \mathbf{w}_{XYZ}\}. \tag{9}$$

The instantaneous error function $\mathcal{E} = \mathrm{tr}(\mathbf{e}^T\mathbf{e})$ can be minimized with respect to $\mathbf{w}_{XYZ}$, to yield a solution for the white point vector, by function minimization routines. Although this represents a sub-optimal solution, it can yield satisfactory results, with little computational load.

White point transformation is extensively used in calibration problems [3]. Since the white point contains information about the spectral qualities of an illuminant, it may model more accurately the degradation process, compared to the other methods presented in this paper. Furthermore, only three parameters should be estimated, which can lead to fast implementations, despite the fact that the transformation $T\{\cdot;\cdot\}$ is nonlinear; lookup tables can be used for this purpose.

E. RBF Approximation

Radial basis functions networks have been used successfully as universal approximators [6], [7]. An arbitrary mapping $f : \mathcal{R}^p \Rightarrow \mathcal{R}$ can be approximated as follows:

$$f(\mathbf{x}) \simeq \sum_{m=1}^{M} w_m \phi(\|\mathbf{x} - \mathbf{t}_m\|) \tag{10}$$

where $\{\phi(\|\mathbf{x} - \mathbf{t}_m\|) \mid m = 1, \ldots, M\}$ is a set of M arbitrary functions, which are known as *radial basis functions*, with corresponding centers $\mathbf{t}_m$ and weights w_m. Of course, if the unknown function is a mapping of the form $f : \mathcal{R}^p \Rightarrow \mathcal{R}^q$, (10) can be utilized to perform approximation on each one of the q dimensions separately. For our purposes, let $\phi(\cdot)$ denote the nonnormalized Gaussian function, i.e.,

$$\phi(\|\mathbf{x} - \mathbf{t}_m\|) = g(\mathbf{x}; \mathbf{t}_m, \mathbf{\Sigma}_m^{-1}) \tag{11}$$

where $\mathbf{\Sigma}_m^{-1}$ represents the inverse covariance matrix of the mth Gaussian and

$$g(\mathbf{x}; \mathbf{t}_m, \mathbf{\Sigma}_m^{-1}) = \exp\left\{-\frac{1}{2}(\mathbf{x} - \mathbf{t}_m)^T \mathbf{\Sigma}_m^{-1}(\mathbf{x} - \mathbf{t}_m)\right\}. \tag{12}$$

Our goal, is the RBF approximation of the unknown function $\mathbf{f} : \mathcal{R}^3 \Rightarrow \mathcal{R}^3$, $\mathbf{s} = \mathbf{f}(\mathbf{x})$. The function $\mathbf{f}$ can also be written as

$$\mathbf{f}(\mathbf{x}) = [f^{(1)}(\mathbf{x}) \quad f^{(2)}(\mathbf{x}) \quad f^{(3)}(\mathbf{x})]^T \tag{13}$$

where $f^{(i)}, i = 1, 2, 3$ is the i-th color component of $\mathbf{f}$. Thus

$$f^{(i)}(\mathbf{x}) \simeq \sum_{m=1}^{M} w_m^{(i)} g(\mathbf{x}; \mathbf{t}_m^{(i)}, \mathbf{\Sigma}_m^{(i)-1}). \tag{14}$$

The parameters of M Gaussian functions should be estimated, for each one of the three color components. Estimation may be performed by a steepest descent algorithm, in order to minimize the total squared error [6]. If the data set size N is large, the computational requirements can be greatly reduced, if the inverse covariance matrix $\mathbf{\Sigma}_m^{(i)-1}$ takes a diagonal form. If the computational cost is still high, the inverse covariance matrix can be set equal to $1/{\sigma_m^{(i)}}^2\mathbf{I}$, where $1/{\sigma_m^{(i)}}^2$ is the variance of the mth Gaussian function for the ith color component. However, these simplifications may limit the overall network restoration performance.

III. SIMULATION RESULTS

The techniques presented in Section II were applied on ten dirty and oxidized Byzantine paintings, in order to assess restoration performance. A representative example is presented here. The use of CIELAB acquisition devices (e.g. spectrophotometers) is not recommended, since they are expensive and have limited spatial resolution which may not be available. A high quality RGB camera

was used for color acquisition. The camera was positioned to point to the center of the painting. The illuminant light beam formed a 45° angle with the painting surface. The experiment described here was carried out on a painting whose right-hand half region was chemically cleaned. Regions of the cleaned and oxidized parts are depicted in Fig. 1. Five regions on each part were selected, with sizes ranging from 5×5 to 16×16 points, depending on the uniformity of the sample. CIEXYZ were obtained from the camera RGB values with the use of a color transformation matrix which corresponds to a reference white with $X = Y = Z = 1$ CIEXYZ tristimulus values [8]. The choice of the specific matrix implicitly defines the illuminant properties. Ten color patches used had size 15×15 pixels, because this number represented fairly well the painting gamut. Sample mean values of each region were estimated and consequently utilized to restore the oxidized image, with the methods described in Section II. Restoration results are depicted in Fig. 1. Subjective evaluation was performed on a number of gamma-corrected SGI workstations. Six restoration experts with no visual impairments were asked to evaluate similarity of the restored images, when compared to the chemically cleaned one. The evaluation was rather easy since the chemically restored right hand part and the digitally restored left part of the painting could be viewed simultaneously. Hardcopies of these images, from a Tektronix Phaser dye sublimation printer, were also produced for comparison and were seen by the experts in the same controlled room light conditions. *Mean opinion scores (MOS)* indicated satisfactory performance, especially for the white point and linear approximation methods, with the former slightly outperforming the latter. Quantitative comparison was performed as well. An estimate of the mean square error $E[(\hat{\mathbf{m}}_{\mathbf{s}} - \hat{\mathbf{m}}_{\hat{\mathbf{s}}})^T(\hat{\mathbf{m}}_{\mathbf{s}} - \hat{\mathbf{m}}_{\hat{\mathbf{s}}})]$ was used as a quantitative criterion for assessing color restoration performance. Results are summarized in Table I.

Subjective evaluation may seem at variance with the claim of good perceptual uniformity of the CIELAB color space, since the RBF method had the second best MSE and the worst perceived quality. This is due to the fact that RBF exhibited good training and poor generalization capabilities. However, the figures of Table I do not reveal the over-fitting characteristics of each method. Thus, the RBF networks used approximated quite well the unknown restoration function at the points of the data set, but could not interpolate satisfactorily. This is not a shortcoming of RBF networks, but rather a consequence of the small data set size used in real-life experiments. On the other hand, white point transformation, and linear approximation yielded good approximation and interpolation performance, due to the underlying "smoothing" nature of each method. Additionally, computational requirements of these two methods is low, in comparison to the RBF. Although sample mean matching exhibited adequate performance in a subset of the image set used, performance was not consistent. This behavior is rather predictable: this approximation method is not characterized by good generalization performance.

Finally, ICP approximation did not produce acceptable results, in terms of visual quality. This should be attributed to the fact that oxidation "moves" color vectors toward the origin (black color), which is an operation that condenses the clean vector space. Since the ICP can not account for scaling between the two vector sets, simulation results were predictable.

The effectiveness of the presented methods, depended strongly on the size of the data used, as well as the size of the color space region they occupied. Of these two factors, the latter one is of the highest significance. If the gamut covered by the available samples is very limited, poor restoration performance will be obtained, regardless of the number of samples used. In particular, this is applicable to the case of sample mean matching. On the other hand, white point transformation is much less dependent on the samples gamut range.

IV. Conclusion

A number of digital restoration techniques that can be used to recover the original appearance of old paintings, with little chemical processing of the paintings' surfaces, were presented in this paper. Simulations performed on a number of different paintings indicated that satisfactory results can be obtained. The best techniques are the linear approximation and the white point transformation. In addition to the advantages mentioned above, all examined methods have small computational requirements. Therefore, they are useful tools to restoration experts and to art historians.

Acknowledgment

The authors would like to thank I. Tavlakis and C. Lotsiopoulos of the 10th Ephorate of Byzantine Antiquities, Thessaloniki, Greece, for the photographic material used in these simulations.

References

[1] G. M. Cortelazzo, G. L. Geremia, and G. A. Mian, "Some results about Wiener-Volterra restoration of the original color quality in old painting imagery," in *Proc. 1995 IEEE Workshop Nonlinear Signal Image Processing (NSIP'95)*, vol. I, Neos Marmaras, Greece, June 1995, pp. 86–89.

[2] G. Wyszecki and W. S. Styles, *Color Science: Concepts and Methods, Quantitative Data and Formulae*, 2nd ed. New York: Wiley, 1982.

[3] H. R. Kang, *Color Technology for Electronic Imaging Devices*. Washington, DC: SPIE Opt. Eng. Press, 1996.

[4] P. J. Besl and N. D. McKay, "A method for registration of 3-d shapes," *IEEE Trans. Pattern Anal. Machine Intell.*, vol. 14, pp. 239–256, Feb. 1992.

[5] C. Vavoulidis and I. Pitas, "Morphological iterative closest point algorithm," presented at the Proc. 7th Int. Conf. on Computer Analysis of Images and Patterns (CAIP'97), Kiel, Germany, Sept. 1997.

[6] S. Haykin, *Neural Networks*. Englewood Cliffs, NJ: Prentice-Hall, 1994.

[7] J. Park and J. W. Sandberg, "Universal approximation using radial basis functions network," *Neural Comput.*, vol. 3, pp. 246–257, 1991.

[8] A. Jain, *Fundamentals of Digital Image Processing*. Reading, MA: Addison-Wesley, 1989.